ISSN 1027-5495. Functional Materials, 26, No.2 (2019), p. 366-374.
doi:https://doi.org/10.15407/fm26.02.366

Liquid steel interaction with MgO-based refractories: A Review

***Abdulaziz Alhussein*[1,2], *Lifeng Zhang*[1], *Alberto N.Conejo*[1,3]**

[1]School of Metallurgical and Ecological Engineering, University of Science and Technology Beijing (USTB), 100083 Beijing, P.R. China
[2]Department of Applied Chemistry, University of Aleppo, Aleppo, Syria
[3]Ferrous Metallurgy Research Institute (FeMRI), Mexico

Received March 7, 2019

The mechanisms of reaction between MgO-based refractories and liquid steel are considered. Conditions are analyzed the formation of a spinel layer at the interface between liquid steel and refractory, the dissolution of refractory materials in liquid steel.
Keywords: steel, magnesia-based refectory, dissolution, reaction, inclusions.

Рассматриваются механизмы реакции между огнеупорами на основе MgO и жидкой сталью. Анализируются условия формирования шпинельного слоя на границе раздела между жидкой сталью и огнеупором, исследуется растворение огнеупорных материалов в жидкой стали.

Взаємодія рідинної сталі з вогнетривами на основі MgO: Огляд. *Abdulaziz Alhussein, Lifeng Zhang, Alberto N.Conejo.*
Розглядаються механізми реакції між вогнетривами на основі MgO і рідкою сталлю. Аналізуються умови формування шпінельною шару на межі розділу між рідкою сталлю і вогнетривом, розчинення вогнетривких матеріалів у рідкій сталі.

1. Introduction

Refractories interact with liquid slag and liquid steel simultaneously and important chemical reactions between those three phases occur [1]. The physical and chemical properties of refractories have an important role in their interaction with slag and steel. Many works have been conducted to understand the dissolution of refractories in liquid slag [2–6], but few works on the interaction between refractory and liquid steel [7, 8]. This situation originates because the chemical attack of liquid slag on refractories can be very intense, depending on the chemical composition of both phases. The chemical attack of liquid steel on the refractory is less intense, however, exists and is a potential source for the formation of nonmetallic inclusions, both endogenous and exogenous. Many kinds of refractory materials have been employed in the continuous casting of steels, such as ladle shrouds, tundish lining, coating refractories, insulating board, nozzle stopper, sliding nozzle, submerged entry nozzle (SEN), etc. These refractories have a large influence on the casting operation and steel quality. Thus, the choice of high-grade refractories should be taken into account [9].

Exogenous inclusions introduced in liquid steel from the dissolution of the refractory may result in loss of the fatigue strength and the destruction of parts operating at elevated loads, since such inclusions may be 5–200 times larger than endogenous inclusions of oxides (reduction products) and sulfides. However, the quantity of macroinclusions in metal on chill casting is so small that they may be detected only by ultrasonic monitor-

ing. The smallest exogenous inclusions, similar in size to large endogenous inclusions, are relatively scarce in metals [10]. Inclusions in steel such as $MgO–Al_2O_3$ spinel are very harmful to the metal forming operations and the quality of steel products [11]. It was reported that complex inclusions such as $MgO–Al_2O_3$, $CaO–MgO–Al_2O_3$, and $CaO–MgO–Al_2O_3–SiO_2$ were observed in the steel when liquid steel contacted with the magnesia-based refractories [12].

The objective of this work is to study the interaction between magnesia-based refractories and liquid steel, explaining the reaction mechanisms that lead to the formation of $MgO{\cdot}Al_2O_3$ spinel.

2. *Reaction between MgO-based refractories and liquid steel*

2.1. MgO refractory

MgO-based refractories are the most common type of refractory material in steelmaking operations. Harada et al. [13] studied the reactions between liquid steel deoxidized by Al and MgO refractory with and without slag additions. It was confirmed that the spinel layer was formed at the steel/MgO refractory interface, and the thickness of the interface layer increased with time. The thickness of the interface layer between liquid steel and the MgO crucible was much smaller than that between liquid steel and the MgO refractory. The formation of $MgO{\cdot}Al_2O_3$ spinel can occur by reactions between the refractory and the slag, and also between liquid steel and the MgO refractory. In aluminum-containing steels, the first step is the reduction of MgO by aluminum dissolved in liquid steel, forming alumina and magnesium, as given in reaction (1). This reaction describes a decrease of dissolved aluminum and an increase of magnesium in the liquid steel, where [ ] is dissolved element in liquid steel:

$$3MgO_{(s)} + 2[Al] = Al_2O_{3(s)} + 3[Mg]. \quad (1)$$

The formation of $MgO{\cdot}Al_2O_3$ spinel can be done by different mechanisms, involving magnesium, aluminum and oxygen dissolved in liquid steel. The first mechanism involves MgO dissolution, as follows:

$$[Mg] + [O] + Al_2O_{3(s)} = MgO \cdot Al_2O_{3(s)}, \quad (2)$$

$$MgO_{(s)} + 2[Al] + 3[O] = MgO \cdot Al_2O_{3(s)}, \quad (3)$$

$$[Mg] + 2[Al + 4[O] = MgO \cdot Al_2O_{3(s)}, \quad (4)$$

The change in standard free energies for reactions (2) through (4) is expressed as follows:

$$\Delta G_2^0 = -110677.14 - 93.52T(J/mol), \quad (5)$$

$$\Delta G_3^0 = -888097.86 - 210.93T(J/mol), \quad (6)$$

$$\Delta G_4^0 = -978094.84 - 128.98T(J/mol). \quad (7)$$

The standard free energy change for reaction (3) is more negative than those for reactions (2) and (4), indicating that the formation of spinel at the steel/refractory interface by reaction (3) is more favorable than reactions (2) and (4) [13–15]. Once the Mg dissolves into the liquid steel, it can react with alumina inclusions, producing spherical spinel inclusions, as given in Eqs. (8) and (9). These reactions take place in the liquid steel regardless the Mg comes from refractory or slag and namely metal-inclusion reaction. The Mg diffusion in the inclusion layer is rate-controlling step [16–18].

$$4Al_2O_{3(s)} + 3[Mg] = 3MgO \cdot Al_2O_{3(s)} + 2[Al], \quad (8)$$

$$Al_2O_{3(s)} + [Mg] + [O] = MgO \cdot Al_2O_{3(s)}. \quad (9)$$

The mechanism for the reduction of MgO by Al was reported by Yang et al. [19], indicating the reaction takes place in two stages. In the first stage, MgO is reduced to form $MgO{\cdot}Al_2O_3$ spinel and magnesium vapor:

$$4MgO_{(s)} + 2[Al] = MgO \cdot Al_2O_{3(s)} + 3Mg_{(g)}. \quad (10)$$

In the second stage, the $MgO{\cdot}Al_2O_3$ spinel is further reduced by Al to produce alumina and magnesium vapor:

$$3[MgO] \cdot Al_2O_{3(s)} + 2[Al] = 4Al_2O_{3(s)} + 3Mg_{(g)}. \quad (11)$$

Many studies [20, 21] have reported that MgO refractory has an obvious effect on the generation of spinel inclusions in Al-killed steel even with a small concentration of dissolved Mg in liquid steel. According to [22, 23] the $(Mn,Mg)O{\cdot}Al_2O_3$ inclusions formed in medium-manganese steel after the formation of $MgO{\cdot}Al_2O_3$ inclusions at the middle stage of ladle furnace (LF) refining. The $(Mn, Mg)O{\cdot}Al_2O_3$ layer was a source of $(Mn, Mg)O{\cdot}Al_2O_3$ inclusions in the liquid steel.

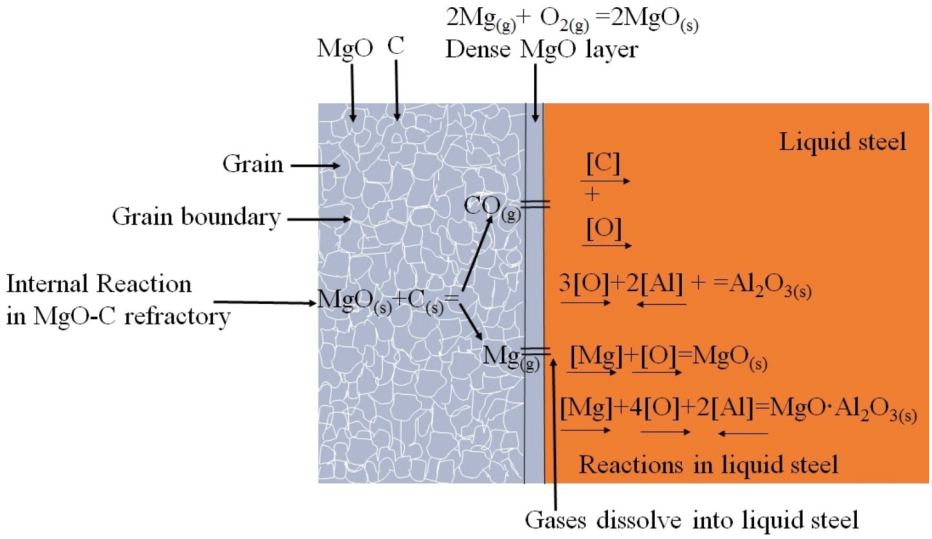

Fig. 1. Theoretical diagram of the reaction between MgO–C refractory and liquid steel.

The reduction of MgO and $MgO{\cdot}Al_2O_3$ refractories by Mn and the standard free energy for each reaction are given in Eqs. (12) through (15), denoting that the standard free energy for $MgO{\cdot}Al_2O_{3(s)}$ + [Mn] reaction is more negative than that for $MgO_{(s)}$ + [Mn] reaction:

$$MgO_{(s)} + [Mn] = MnO_{(s)} + [Mg], \quad (12)$$

$$\Delta G^{o}_{12} = -198125 - 210.24T(\text{J/mol}), \quad (13)$$

$$[MgO] \cdot Al_2O_{3(s)} + [Mn] = MnO \cdot Al_2O_{3(s)} + [Mg]. \quad (14)$$

$$\Delta G^{o}_{14} = -235312 - 231.58T(\text{J/mol}). \quad (15)$$

Deng et al. [18] investigated the effect of Al_2O_3, MgO, $MgO{\cdot}Al_2O_3$ refractories on the formation of inclusions in the secondary steelmaking. Only MgO formed $MgO{\cdot}Al_2O_3$ spinel, but depending on the oxygen activity in steel. They investigated two cases with low and high oxygen activity, 1 and 500 ppm O, respectively. $MgO{\cdot}Al_2O_3$ spinel formed only when the activity of oxygen was low. The reduction of MgO into Mg and O requires reducing conditions, then the spinel can be formed combining reaction (16) with reaction (1), (3) and (7):

$$[Mg] + [O] = MgO_{(s)}. \quad (16)$$

If the oxygen potential is high, then the activity of Mg is extremely low and alumina cannot be transformed into $MgO{\cdot}Al_2O_3$ spinel. It was reported that the Mg for spinel generation mainly came from the reaction between steel and slag rather than from the reaction between steel and refractory based on industrial scale investigations. Spinel inclusions can be modified to liquid inclusions by a calcium treatment [24].

2.2. MgO–C refractory

Carbon in MgO–C refractories is critical to improve refractory life. Carbon decreases wetting between the liquid slag and the refractory, however, it can dissolve in the liquid steel and affect the final chemical composition of the steel. The investigation of carbon pickup of steel from refractories containing carbon is of great commercial significance, in particular for Ultra-low carbon (ULC) steel [25]. The mechanism of the reaction between MgO–C refractory material and aluminium deoxidized liquid steel has been extensively investigated. The mechanism of the reaction between MgO–C refractory and steel takes place in four steps [8, 26–31]:

Step 1: An internal reaction between the MgO and C is occurred to generate magnesium vapor and CO gas:

$$MgO_{(s)} + C_{(s)} = Mg_{(g)} + CO_{(g)}. \quad (17)$$

This reaction is driven by the difference of partial pressure of gases from the equilibrium partial pressure; the equilibrium partial pressures depend on the total pressure and the refractory composition.

Step 2: $Mg_{(g)}$ diffuses towards the refractory/liquid steel interface where it encounters a higher oxygen potential and is oxi-

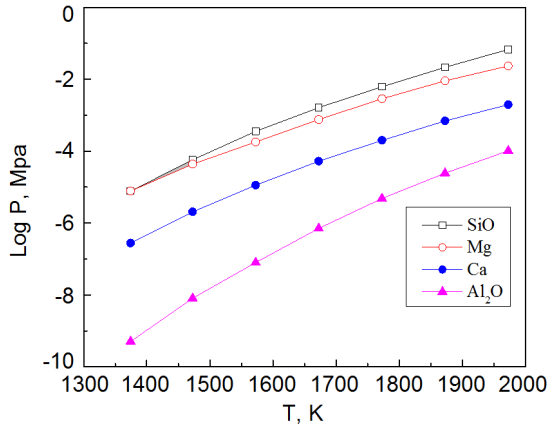

Fig. 2. Effect of temperature on equilibrium partial pressure of SiO, Mg and Al_2O_3 [8].

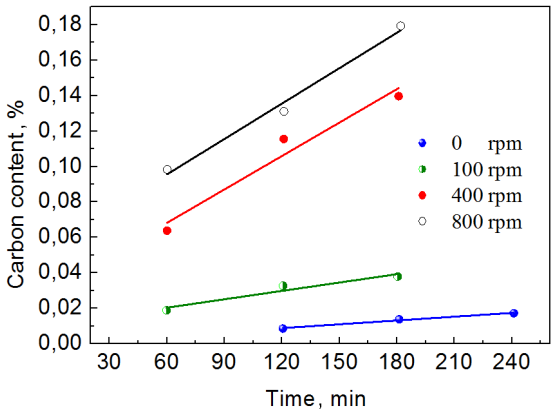

Fig. 3. Change in the content of *C* in 0.1 Al-killed steel as a function of rotation speed and time 1600°C [28].

dized to MgO, forming an MgO dense layer, Eq. (18):

$$2Mg_{(g)} + O_{2(g)} = 2MgO_{(s)}. \quad (18)$$

Step 3: Simultaneously, the $CO_{(g)}$ diffuses to the refractory/liquid steel interface where it is dissolved in the liquid steel according to the following reaction:

$$CO_{(g)} = [C] + [O]. \quad (19)$$

The dissolution of $CO_{(g)}$ into the liquid steel according with will enhance the dissolution of MgO according with Eq. (17).

Step 4: Dissolved Al, Mg and O react, forming Al_2O_3 and MgO or mixtures of them as given in Eqs. (4), (16) and (20):

$$2[Al] + 3[O] = Al_2O_{3(s)}. \quad (20)$$

The mechanism of the reaction between the MgO–C refractory and liquid steel is illustrated in Fig. 1.

In addition to the reaction between carbon and MgO, carbon can react with other oxides in the refractory such as SiO_2, Al_2O_3 and CaO, producing gases such as SiO, Al_2O and Ca at the interface:

$$SiO_{2(s)} + C_{(s)} = CO_{(g)}. \quad (21)$$

$$Al_2O_{3(s)} + C_{(s)} = Al_2O_{(g)} + CO_{(g)}. \quad (22)$$

$$CaO_{(s)} + C_{(s)} = Ca_{(g)} + CO_{(g)}. \quad (23)$$

Based on thermodynamics, the occurrence of reactions (21) to (23) depends on the partial pressure of Mg, SiO, Al_2O and Ca, as shown in Fig. 2. The Mg and SiO gases are the most readily formed. However, it was found that the equilibrium partial pressures increase in the order $P_{Al2}O < P_{Ca} < P_{Mg} < P_{SiO}$ and that the Mg and SiO gases are the most readily formed thermodynamically [8].

The effect of MgO–C refractory on the formation kinetics of $MgO{\cdot}Al_2O_3$ spinel in the extra-low oxygen steel was investigated on a laboratory scale by inserting a MgO–C refractory rod into the Al-killed liquid steel. The results showed that the Al_2O_3 inclusions gradually transformed into $MgO{\cdot}Al_2O_3$ spinel by increasing the reaction time and the final MgO inclusion was in equilibrium with the MgO–C refractory [32]. It was confirmed that the dissolution rate increased with increasing steel temperature, rotation speed and immersion time. The decrease in the aluminium content in steel was due to the reaction of Al in the melt with C and MgO in the refractory at the interface. The overall reaction is expressed by Eq. (24):

$$3MgO_{(s)} + 3C_{(s)} + 2[Al] = Al_2O_{3(s)} + 3Mg_{(g)} + 3[C]. \quad (24)$$

The effect of the rotation speed on the dissolution of MgO–C refractory to liquid steel is shown in Fig. 3 [28]. Liu et al. [33] investigated the dissolution behavior of Mg from MgO–C refractory in Al-killed liquid steel. They concluded that both Al and C can reduce MgO from the MgO–C refractory, resulting in an increase in Mg content in the liquid steel. However, the effect of C on the reduction of MgO was negligible when C content in MgO–C was less than 10 %, and the reduction of MgO occurred only by Al.

Cirilli et al. [7] and Kwon et al. [34] reported that the reduction of refractory

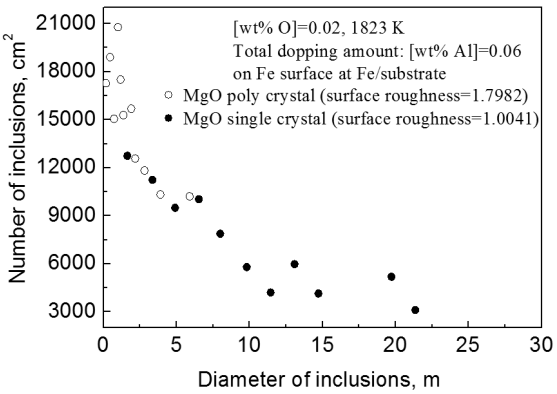

Fig. 4. Effect of surface roughness of MgO on size distribution of inclusion particles [35].

oxides by carbon in the refractory led to change in the rate of C dissolution when the refractory contacted with the steel at a high temperature. Lee et al. [35] investigated the effect of surface roughness of MgO substrate on the size distribution of inclusions. It was found that the surface roughness of refractory activated the interfacial reactions between the liquid steel and the MgO substrate, increasing the number of inclusions and reducing the diameter of particles, as shown in Fig. 4. Thus, the use of lower roughness of refractories should be considered to improve steel cleanliness.

2.3. MgO–SiO_2 refractory

Steel reoxidation in the tundish reactor occurs in three ways: 1) infiltration of air into the liquid steel, which could be prevented by using a tundish cover powder and tundish slag; 2) interactions between the liquid steel and the slag; 3) interactions between the liquid steel and refractories [36]. The existence of SiO_2 in tundish refractory causes strong reactions with deoxidizing elements in the liquid steel, resulting in the detaching of large particles from the steel/refractory interface to the molten liquid. The detached particles would react with deoxidizing elements leading to change in their composition in steel [37]. An example of the strong reaction produced by the reaction between the liquid steel and the tundish refractory is shown in Fig. 5. A layer of $MgO{\cdot}Al_2O_3$ spinel at the steel/tundish refractory was formed due to the transformation of the $2MgO{\cdot}SiO_2$ phase in the tundish refractory materials by the Al, as expressed in Eq. (25):

$$3(2MgO \cdot SiO_2)_{(s)} + 4[Al] = \quad (25)$$
$$= 2MgO \cdot Al_2O_{3(s)} + 2MgO_{(s)} + 3[Si].$$

The composition of the interface layer and its physical state change based on the initial chemical composition of refractories. Reaction (25) does not affect the steel cleanliness due to a substitution of SiO_2 by Al_2O_3 in the refractory, however, the separation of spinel particles or layers from the interface can influence negatively the steel cleanliness [38–41].

Li et al. [42] studied the effect of MgO based castables containing 0–7 % microsilica on oxygen content of IF (interstitial free) steel. They concluded, as the content of microsilica in based castables increased from 0 to 3 %, the total oxygen in IF steel increased, due to the dissolution of MgO and SiO_2 in liquid steel. When the content of microsilica in MgO based castables increased from 3 to 7 %, the total

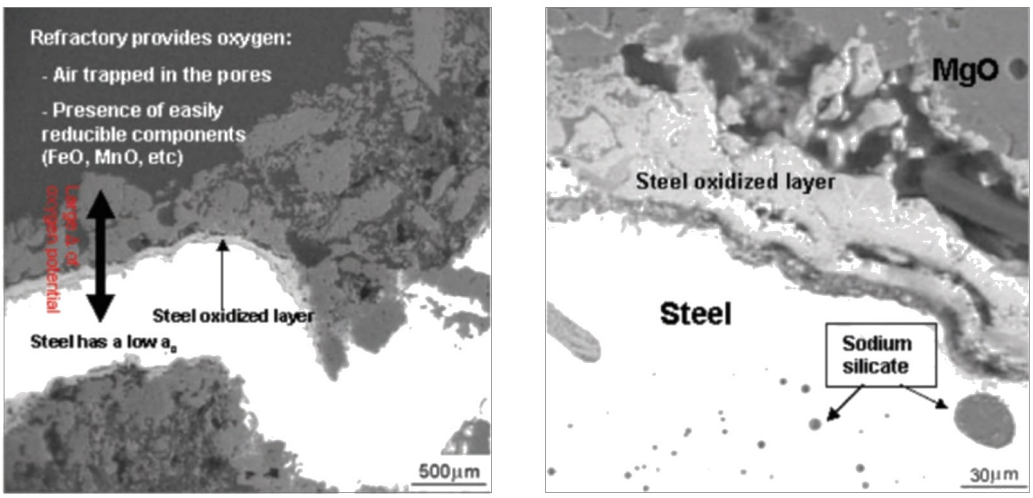

Fig. 5. SEM image of the steel/refractory interface indicating steel oxidized layer [38].

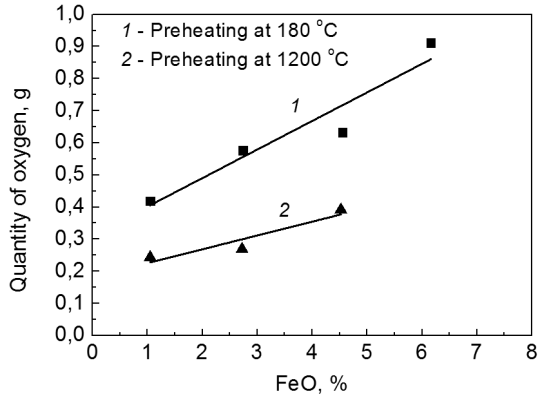

Fig. 6. Content of picked up oxygen (caught by aluminum) in steel as a function of the FeO content in the tundish refractory [43].

oxygen in IF steel decreased. This was due to the formation of a viscous liquid layer between the liquid steel and the refractory. The liquid layer prevented direct dissolution of the oxygen and metal atoms in the liquid steel. Once the liquid layer formed, the transport of the oxygen from the refractory to the liquid steel was occurred by an interface reaction between the liquid layer and the refractory, and then a further interface reaction between the liquid layer and the liquid steel.

Lehmann et al. [43] confirmed that the liquid steel reoxidation by the tundish refractory materials increased with decreasing the content of MgO in the tundish refractory. This was because of the increase in the content of FeO and SiO_2 in the refractory. The oxygen pick up by the liquid steel increased with increasing the content of FeO and SiO_2 in the refractory. The relationship between the content of picked up oxygen in steel and the FeO in refractory is illustrated in Fig. 6. It was recommended that the content of the MgO in tundish refractory should be higher than 75 % to minimize the liquid steel reoxidation by the tundish working refractory. In addition, it was shown that the water content is an important aspect. Refractories fired at 1200°C before put in contact with liquid metal provide less reoxidation than refractories simply dried at 180°C.

Muxing et al. [44] and Yan et al. [45] studied the interaction between the steel and distinct gunning materials in the tundish. They reported there were three phenomena: (1) the liquid steel was infiltrated into the gunning material; (2) the refractory was eroded and large inclusions with similar composition as gunning material were found in the steel close to the steel/refractory interface; (3) the steel was reoxidized and a FeO_x layer with a thickness of 5–30 μm was formed at the steel/refractory interface. The formation of the FeO_x layer was due to the large difference of oxygen potential between the refractory and the steel. Because of the low oxygen potential in the furnace atmosphere (around 10^{-16} atm) and the dissolved Al and Ti, the liquid steel had a low content of dissolved oxygen. The refractory could be considered as a potential oxygen provider.

2.4. MgO–SiC refractory

It has been reported that MgO–SiC and Al_2O_3–SiC, used in slag line, cause carbon pick up by the liquid steel [25, 46]. Interactions between the MgO–SiC refractory and the liquid steel were investigated by electron probe microanalysis (EPMA) with energy dispersive spectrometer (EDS). Fig. 7 represents the influence of the interactions on the MgO–SiC refractory and Table lists the chemical composition of selected areas in

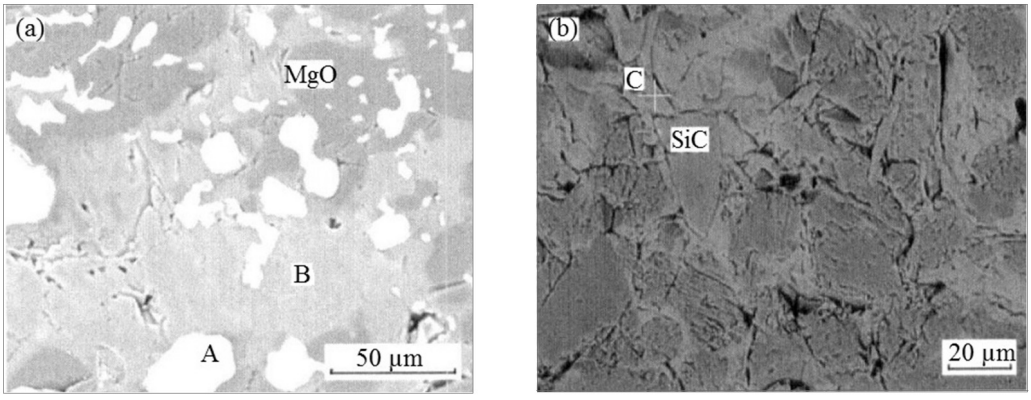

Fig. 7. EDM analysis on the hot face of Mg–SiC refractory [47].

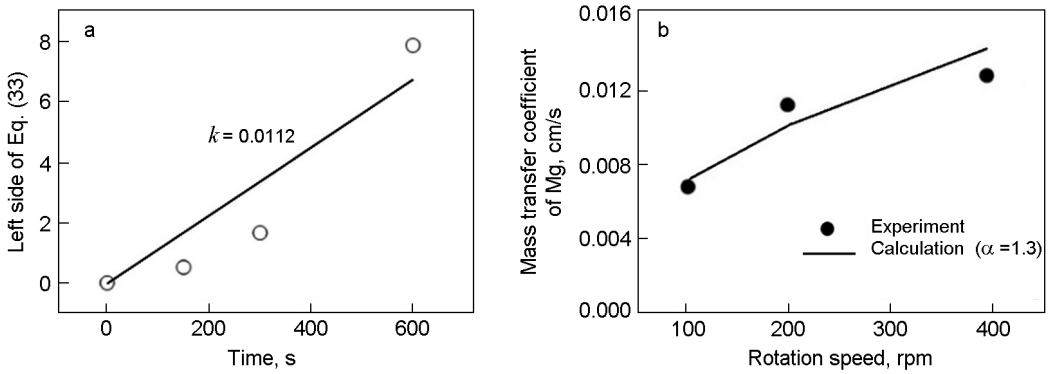

Fig. 8. Estimation of the mass transfer coefficient for Fe–0.3 %Al liquid steel at a rotation rate of 200 rpm (a) and mass transfer for Fe–0.3 %Al liquid steel as a function of rotation speed (b) [13].

Fig. 7. It could be seen from Fig. 7(a) that the FeSi is formed in the hot face of refractory. Fe is supplied from the IF steel and silicon from the refractory because the silicon content in the FeSi was much higher than that in the IF steel specimen, indicating that Si from the SiC dissolved into the liquid steel. Several oxides consisted of MgO, CaO, Al_2O_3, and SiO_2 could be seen in this area, which might be liquid mixtures at high temperature. The SiC in the refractory was oxidized to SiO_2 during the heating process. The generated SiO_2, which formed a layer around SiC particles, protected the inner SiC particle from oxidation. The chemical reactions of the dissolution of SiC in MgO–SiC refractory into the liquid steel are given as follows:

$$2SiC_{(s)} + 3O_{(2g)} = 2SiO_{2(s)} + 2CO_{(g)}, \quad (26)$$

$$2SiO_{(2s)} = [SiO] + [O], \quad (27)$$

$$3SiO_{(2s)} + 4[Al] = 2Al_2O_{3(s)} + 3[Si]. \quad (28)$$

The change in standard free energies for the reactions (26) through (28) is expressed in Eqs. (29) through (31), respectively:

$$\Delta G^o_{26} = -630900 + 49.78T(\text{J/mol}), \quad (29)$$

$$\Delta G^o_{27} = -580550 - 220.66T(\text{J/mol}), \quad (30)$$

$$\Delta G^o_{28} = -720680 + 133T(\text{J/mol}). \quad (31)$$

The change in standard free energy for reaction (28) is much lower than that for reaction (27), so the Si pick-up from the refractory surface proceeds according to Eq. (28). Then, the inner SiC would dissolve into the liquid steel immediately after the SiO_2 film was broken, allowing the exposure of inner SiC particle to the liquid steel [47].

Table. Chemical composition of selected area A, B and C in Fig. 7 [47]

Point	Fe, %	Si, %	Mg, %	Al, %	Ca, %	O, %
A	93.42	6.58	–	–	–	–
B	–	4.62	16.89	5.73	23.62	62.09
C	–	29.12	22.59	–	9.60	38.69

3. *Kinetics of the dissolution of magnesia-based refractory into the liquid steel*

The magnesium mass transfer from the MgO refractory into the liquid steel can be represented by a first order kinetics:

$$J_{Mg} = k\left(C_{Mg^*} - C_{Mg}\right), \quad (32)$$

where J_{Mg} is the molar flux of Mg (mol/m^2·s), k is the mass transfer coefficient of Mg (m/s), and C^*_{Mg} and C_{Mg} are the molar concentration of Mg in liquid metal at the interface and bulk (mol/m^3), respectively. Eq. (33) is obtained after rewriting and integration of Eq. (32):

$$\left(\frac{w}{A\rho_m}\right)\ln\frac{[\%Mg]^* - [\%Mg]^0}{[\%Mg]^* - [\%Mg]} = kT, \quad (33)$$

where $[\%Mg]^*$, $[\%Mg]^0$ and $[\%Mg]$ are the mass concentrations of Mg at the interface and in the bulk at time 0 and t, respectively (%), t is time (s), A is the interface area between the liquid steel and the MgO refractory (m^2), ρ_m is the density of liquid steel (kg/m^3) and W is the weight of liquid steel (kg). The mass transfer can be estimated based on the relationship between the left-side term of Eq.

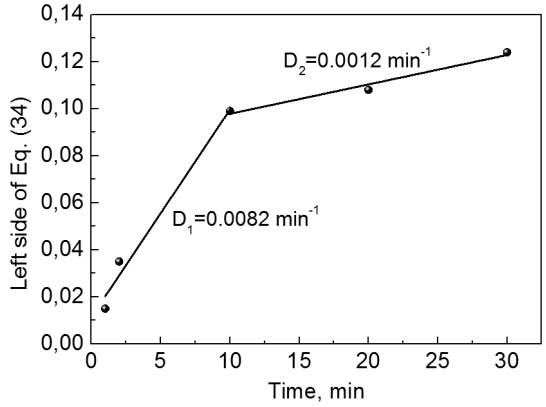

Fig. 9. Relationship between the left side of Eq. (34) and time at 1550°C [41].

(33) and t, as shown in Fig. 8a, according to Harada et al. [13] results. Meanwhile, It was found that the mass transfer of Mg was increased with increasing the rotation speed as shown in Fig. 8b.

The degradation of refractory materials can be caused by strong reactions between liquid steel containing aluminium and MgO-based refractory. In this case, the dissolution rate could be estimated to describe the reaction between liquid metal and refractory using Eq. (34), where the term $kA\rho_m/W$ in Eq. (33) is the total dissolution rate D (s^{-1}) of silica in $MgO–SiO_2$ based refractory material. Due to the deviations in the Mg content in Fe–Al alloy, which resulted by an inhomogeneous distribution of separated layers and particles from the interface to the liquid Fe–Al alloy, the dissolution rate was calculated for silica as shown in Fig. 9. This figure shows two rates. For the first rate, the variation in the dissolution rate of the refractory was due to a large increase in the interfacial area in the first range of the reaction time by degrading the refractory material as a dominating factor. Later the increase in the spinel layer thickness at the interface increased the reaction resistance for silica reduction in the bulk and seemed to be a dominating factor [41].

$$\ln\frac{[\%Si]^* - [\%Si]^0}{[\%Si]^* - [\%Si]} = Dt. \qquad (34)$$

Another way to estimate the mass transfer coefficient of solid material into the liquid metal is to rotate the solid sample in the liquid metal. Then, the mass transfer coefficient of metal could be calculated by Eq. (35):

$$(r_0 - r_t)\frac{100\rho_r}{\rho_s\Delta[\%M]} = k\Delta t, \qquad (35)$$

where r_0 and r_t are the radius of the refractory sample before and after the reaction (m), respectively, ρ_r and ρ_s are the densities of the refractory sample and the liquid metal (kg/m^3), respectively, $\Delta[\%M]$ is the concentration difference between the saturation and the initial concentration of M in liquid metal and k is the mass transfer coefficient of M (m/s) [48]. The coupled reaction model can be used to calculate reactions between the liquid steel and the MgO refractory [49, 50].

4. Conclusions

The interaction between liquid steel and the refractory should always be taken into account in order to improve the steel cleanliness and the refractory life. This interaction is responsible for the formation of $MgO{\cdot}Al_2O_3$ spinel inclusions in steel.

The mechanism of reactions between liquid steel and the MgO-based refractory depends on the chemical composition of steel and refractory.

Carbon in the MgO–C refractory can enhance its dissolution rate. This phenomenon can be avoided using high purity MgO refractories.

Acknowledgements. The authors are grateful for support from the University of Science and Technology Beijing (USTB), China (Grant No. 06500108), the Laboratory of Green Process Metallurgy and Modeling (GPM2) at the School of Metallurgical and Ecological Engineering at University of Science and Technology Beijing (USTB), China, Chinese Government Scholarship (CSC No. 2015760010), China.

References

1. N.Sutucliffe, in: Proc. Int. Conf. on Molten Slags Fluxes and Salts. VII (2004), p.423.
2. S.Riaz, A.Cederlund-losenborg, K.C.Mills, K.Bain, in: Proc. 6th Intern. Conf. on Molten Slags, Fluxes and Salts (2000), p.6.
3. G.J.Hassall, K.G.Bain, N.Jones, M.O.Warman, *Ironmak. Steelmak.*, **29**, 383 (2002).
4. P.T.Jones, B.Blanpain, P.Wollants et al., Proc. 6th Intern. Conf. Molten Slags, Fluxes and Salts. Dept..Mater. Scie. Engin., KTH, Sweden, (2000).
5. K.Beskow, N.N.Tripathi, M.Nzotta et al., *Ironmak. Steelmak*, **31**, 514 (2004).
6. S.A.Nightingale, B.J.Monaghan, G.A.Brooks, *Metal. Mater. Trans. B*, **36**, 453 (2005).

7. F.Cirilli, D.A.Di, P.Dupel, P.Guillo, in: Proc. 6th Intern. Conf. Molten Slags, Fluxes and Salts (2000).
8. V.Brabie, *Steel Res.*, **68**, 54 (1997).
9. S.Yoshino, H.Kyoden, Y.Namba, *Iron Steelmaker*, **7**, 16 (1980).
10. L.A.Moiseeva, B.P.Moiseev, *Steel in Translation*, **37**, 607 (2007).
11. J.H.Park, D.S.Kim, *Metal. Mater. Trans. B*, **36**, 495 (2005).
12. M.Jiang, X.Wang, J.Pak, P.Yuan, *Metal. Mater. Trans. B*, **45**, 1656 (2014).
13. A.Harada, G.Miyano, N.Maruoka et al., *ISIJ Int.*, **54**, 2230 (2014).
14. H.Matsuno, Y.Kikuchi, *Tetsu-to-Hagane*, **88**, 48 (2002).
15. H.Itoh, M.Hino, S.Ban, *Tetsu-to-Hagane*, **84**, 85 (1998).
16. G.Okuyama, K.Yamaguchi, S.Takeuchi, K.Sorimachi, *ISIJ Int.*, **40**, 121 (2000).
17. Y.Sun, Y.Zeng, R.Xu, K.Cai, *Int. J. Miner. Metal., Mater.*, **21**, 1068 (2014).
18. Z.Deng, M.Zhu, S.Du, *Metal. Mater. Trans. B*, **47**, 1 (2016).
19. J.Yang, T.Yamasaki, M.Kuwabara, *ISIJ Int.*, **47**, 699 (2007).
20. Y.G.Chi, Z.Y.Deng, M.Y.Zhu, *Steel Res. Int.*, **88**, 1600470 (2017).
21. Z.Deng, M.Zhu, *ISIJ Int.*, **53**, 450 (2013).
22. L.Kong, Z.Deng, M.Zhu, *ISIJ Int.*, **57**, 1537 (2017).
23. L.Kong, Z.Deng, M.Zhu, *Metall. Mater. Trans. B*, **47**, 3158 (2016).
24. N.Verma, P.C.Pistorius, R.J.Fruehan et al., *Metal. Mater. Trans. B*, **43**, 830 (2012).
25. G.Ruan, N.Li, *Ironmak. Steelmak*, **31**, 342 (2004).
26. J.Elliott, *Electric Furnace Proceedings*, **29**, 12 (1971),
27. G.D.Pickering, J.D.Batchelor, *Amer. Ceram. Soc. Bull.*, **50**, 611 (1971).
28. S.Jansson, V.Brabie, P.Jonsson, *Ironmak. Steelmak.*, **35**, 398 (2006).
29. N.Ahmadi, M.Hirasawa, M.Sano, *ISIJ Int.*, **36**, 1366 (1996).
30. F.Cirilli, M.Tonelli, *Steel Res. Int.*, **77**, 250 (2006).
31. A.Watanabe, H.Takahashi, F.Nakatani, *J. Amer. Ceram. Soc.*, **69**, C (1986).
32. C.Liu, F.Huang, J.Suo, X.Wang, *Metall. Mater. Trans. B*, **47**, 989 (2016).
33. C.Liu, X.Gao, S.Kim, S.Ueda, S.Kitamura, *ISIJ Int.*, **58**, 488 (2018).
34. O.D.Kwon, C.H.Yim, C.H.Rhee, in: UNITECR'01. Proc. Unified Int. Tech. Conf. on Refractories. 7th Biennial Worldwide Congress, **1**, 252 (20010)
35. Y.Lee, S.Jung, D.Min, *Ironmak. Steelmak.*, **41**, 213 (2014).
36. K.Sasai, Y.Mizukami, *ISIJ Int.*, **40**, 40 (2000).
37. J.Simoes, D.Janssen, CFI, GOLLER VERLAG GMBH ASCHMATTSTRASSE 8, D-76532 BADEN BADEN, Germany, **85**, E86 (2008).
38. M.Mantovani, L.Moraes, R.Leandro da Silva et al., *Ironmak. Steelmak.*, **40**, 319 (2013).
39. H.Jungblut, T.Scherrmann, in: Proc. of 3rd European Conference on Continuous Casting, Madrid (1988), p.707.
40. N.Bannenberg, H.Lachmund, METEC Congress 94. 2nd European Continuous Casting Conference. 6 th International Rolling Conference, **1**, 25 (1994).
41. A.Alhussein, P.R.Scheller, W.Yang, *Metall. Res. Technol.*, **115**, 1 (2018).
42. H.Li, Y.Wei, *Br. Ceram. Trans.*, **102**, 175 (2003).
43. J.Lehmann, M.Boher, M.Kaerle, *CIM Bull.*, **90**, 69 (1997).
44. M.Guo, M.Van Ende, P.T.Jones et al., in: Proc. of AIST Proceedings, Association for Iron and Steel Technology, 2, 621 (2009).
45. P.Yan, M.Van Ende, E.Zinngrebe et al., *ISIJ Int.*, **54**, 2551 (2014).
46. N.Bannenberg, in: Proc. of UNITECR'95 Proceedings, 1, 37 (1995).
47. Y.Wei, L.Nan, X.Chen et al., *J. Iron Steel Res. Int.*, **15**, 92 (2008).
48. Y.Wei, C.Weiqing, Y.Yindong et al., in: Proc. of AISTech 2015 Proceedings (2015), p.2162.
49. S.Taira, K.Nakashima, K.Mori, *ISIJ International*, **33**, 116 (1993).
50. S.Y.Kitamura, H.Shibata, N.Maruoka, *Steel Res. Int.*, **79**, 586 (2008).